Thermodynamic properties of inverse power fluids

A. C. Brańka*
Institute of Molecular Physics, Polish Academy of Sciences, Smoluchowskiego 17, 60-179 Poznań, Poland

D. M. Heyes†
Chemistry Division, School of Biomedical and Molecular Sciences, University of Surrey, Guildford GU2 7XH, United Kingdom

(Received 1 June 2006; published 13 September 2006; publisher error corrected 21 September 2006)

The local scaling behavior of the radial distribution function of the soft sphere or inverse power, r^{-n} potential, fluid leads to a formula for the equation of state. From this formula different analytic forms for the compressibility factor, Z, have been derived. In the first, Z is expressed as a product of three functions, the hard sphere equation of state and two other functions incorporating the effects of the potential softness. In the second formula, the compressibility factor is cast in terms of the position and height of the first peak in the radial distribution function. In the final form, Z can be expressed as an exponential function which depends entirely on a combination of the virial coefficients. In each case Z is an explicit expression which has the correct low density limiting behavior and is accurate up to the freezing density for all packing fractions and *circa* $n \geqslant 12$. Expressions are derived for the various component functions required for the different forms of Z, and relations between them are established. The compressibility factor manifests a maximum value or "ridge" when plotted as contours on the density-softness plane. It starts for the softer fluids at lower densities, increases with particle stiffness, and crosses the freezing line at $n \cong 33$. From the compressibility factor other thermodynamic quantities can be obtained and the density-softness dependence of the infinite frequency limit elastic properties been determined. A self-consistent expression is derived for the effective hard sphere packing fraction (or equivalently, diameter), valid for all packing fractions and *circa* $n > 12$. The effective hard-sphere diameter is compared with the formulas of Barker and Henderson, and Wheatley.

DOI: 10.1103/PhysRevE.74.031202 PACS number(s): 61.20.−p, 64.10.+h, 05.20.Jj, 05.70.Ce

I. INTRODUCTION

This work is concerned with the properties of a classical system of particles interacting through the repulsive soft-sphere or inverse-power potential,

$$u(r) = \epsilon\left(\frac{\sigma}{r}\right)^n, \tag{1}$$

where r is the separation between two particles, σ is the particle diameter, ϵ sets the energy scale, and n is a parameter determining the potential steepness (the softness is $\varepsilon = n^{-1}$). This pair potential possesses some useful properties, in that, for example, excess thermodynamic properties do not depend upon the density and temperature separately but on a dimensionless combination of the two, a temperature-scaled density $\tilde{\rho} = (\beta\epsilon)^{3/n}\rho\sigma^3$, where $\rho = N/V$ is the number density and $\beta = 1/k_BT$ with k_B Boltzmann's constant and T is the temperature [1]. Therefore for a given n, the entire phase behavior or $T-\rho$ plane can be determined by performing computations along a single isotherm or isochore. Furthermore, several basic physical properties of a system of inverse-power particles are trivially related to each other, e.g., pressure and mechanical properties are directly related to the interaction energy per particle [2]. Thus, for any n, a common theoretical treatment for the static properties is possible, which is not possible for other potentials, such as Lennard-Jones. The self-similarity of the soft-sphere potential also has the consequence that uniform scaling of the particle coordinates simply scales the magnitude, but not the structure of the potential energy landscape [3].

This potential, with $n=12$, has been used as a reference fluid in a perturbation theory of liquids [4,5]. Also the inverse power system for $n \gg 1$ provides an alternative approach to the properties of system of the hard sphere system, being the limiting case when $n \to \infty$ [6–8]. A wide spectrum of practically important systems from the very soft to the extremely hard can be considered by changing the stiffness parameter, n. Systems that could be represented approximately by such a potential include microgels [9,10], granular systems [11], and colloidal liquids [12]. The practical usefulness of the inverse-power system relies on having direct access to properties of the system at any point in the density-softness plane. An understanding and detailed knowledge of thermodynamic properties in the density-softness plane would make it more useful as a reference for physical systems.

Recently, a new feature of the inverse-power system has been demonstrated [13]. It was shown that, in such a system, there exists a local scaling of structural properties which can be used to obtain a general formula for the equation of state. This work concentrates on establishing an accurate analytic representation for the equation of state in the density-softness fluid plane. For the first time a detailed and clear assessment of the role of the "softness" parameter is possible. Other consequences of the local scaling property are considered, such as the existence of new relations involving thermodynamic or structural parameters. The main aim of the work is the derivation of a comprehensive quantitative

*Electronic address: branka@ifmpan.poznan.pl
†Electronic address: d.heyes@surrey.ac.uk

description of thermodynamic properties of the inverse-power system in the entire fluid phase.

The general equation of state formulas are described in Sec. II. The form of the component W function is presented in Sec. III, and the density-softness plane is analyzed in Sec. IV. In Sec. V the explicit forms of the remaining component functions are established. In Sec. VI examples of the consequences of the scaling property are discussed. An essentially exact formula for the effective packing fraction or effective diameter is derived from the equation of state in Sec. VII. Concluding remarks are made in Sec. VIII.

II. THEORY

Because of the scaling properties of the r^{-n} potential it is possible and convenient to perform calculations in the following reduced units: $\tilde{r}=r\sigma^{-1}(\beta\epsilon)^{-1/n}$, $\tilde{u}=\beta u=\tilde{r}^{-n}$, and $\tilde{P}=P\epsilon^{-1}\sigma^3(\beta\epsilon)^{1+(3/n)}$. Also a temperature-scaled packing fraction, $\tilde{\zeta}=\pi\tilde{\rho}/6$, is used to characterize the density of the system. In this work we omit the tilde, so keep in mind that we are referring to temperature-scaled quantities below.

Recently we showed that, at least for $n \geqslant 18$, the cavity or indirect correlation function, $y(r)=g(r)\exp(\beta u)$, can be well-represented in the particle contact region by the power or algebraic function,

$$y(r) = \exp(A)r^{-C} \tag{2}$$

where A and C are functions of n and ζ [13]. With this form of the cavity function the general formula for the equation of state of the inverse power fluid is,

$$Z(\zeta,n) = \frac{P}{\rho} - 1 = 4\zeta\Gamma[1+(C-3)/n]e^{A}. \tag{3}$$

Note that in this definition of the compressibility factor, Z the kinetic contribution has been subtracted off. In the above equation, $\Gamma(x)$ denotes the gamma function of x [14]. Both $A(\zeta,n)$ and $C(\zeta,n)$ are regular (smooth, monotonic, finite) functions with a well-defined form in the limit $n\to\infty$. This permits the formula in Eq. (3) to be expressed in terms of the hard-sphere equation of state, Z_{HS},

$$Z(\zeta,n) = Z_{HS}(\zeta)\Gamma[1+(C-3)/n]e^{\delta A}. \tag{4}$$

In the above equation, $Z_{HS}=P_{HS}/\rho-1=4\zeta\exp(A_{HS})$. Also $\delta A=A-A_{HS}$, where A_{HS} stands for $A(\zeta,n\to\infty)$. For Z_{HS}, there are several accurate analytical representations in the literature [15], for example, the Carnahan and Starling (CS) formula [16], or that of Kolafa [17]. Therefore it is sufficient to concentrate on the functions $\delta A(\zeta,\varepsilon=1/n)$ and $C(\zeta,\varepsilon=1/n)$, which determine the remaining soft parts of the equation of state of Eq. (4). This form of the equation of state has been discussed in [13]. Consideration of Z_{HS} reveals some advantages of Eq. (4) compared with the generic formula (3), e.g., in giving an accurate and simple representation of the equation of state for larger n. Note however, that the softer system fluids are thermodynamically stable in regions where the hard sphere fluid is metastable, and so there is no well defined Z_{HS} and it becomes difficult to provide a physical meaning to δA in that case.

Importantly, it was shown that for any n the function A is smooth and monotonically increasing with ζ and $A(\zeta=0,\varepsilon)=0$. Thus, it is reasonable to express the A function as a power series,

$$A(\zeta,n) = \sum_{k=1}^{\infty} a_k(n)\zeta^k. \tag{5}$$

With this form for A the virial expansion can be exploited. Expanding the right-hand side of Eq. (3) and comparing with the virial expansion $Z=\mathcal{B}_2\zeta+\mathcal{B}_3\zeta^2+\mathcal{B}_4\zeta^3+\cdots$ the a coefficients can be expressed in terms of the virial coefficients and the gamma function derivatives. They have the general form $a_k=w_k-\frac{1}{k!}\partial^k\psi/\partial\zeta^k$, where $\psi=\ln[\Gamma(1+(C-3)\varepsilon)]$, and the $w_k(\varepsilon)$ terms are combinations of the virial components of the soft particle system, which for the first five cases is,

$$w_1 = \mathcal{B}_3^*, \tag{6}$$

$$w_2 = \mathcal{B}_4^* - \frac{1}{2}\mathcal{B}_3^{*2}, \tag{7}$$

$$w_3 = \mathcal{B}_5^* - \mathcal{B}_4^*\mathcal{B}_3^* + \frac{1}{3}\mathcal{B}_3^{*3}, \tag{8}$$

$$w_4 = \mathcal{B}_6^* - \mathcal{B}_5^*\mathcal{B}_3^* + \mathcal{B}_4^*\mathcal{B}_3^{*2} - \frac{1}{2}\mathcal{B}_4^{*2} - \frac{1}{4}\mathcal{B}_3^{*4}, \tag{9}$$

$$w_5 = \mathcal{B}_7^* - \mathcal{B}_6^*\mathcal{B}_3^* - \mathcal{B}_5^*\mathcal{B}_4^* + \mathcal{B}_5^*\mathcal{B}_3^{*2} + \mathcal{B}_4^{*2}\mathcal{B}_3^* - \mathcal{B}_4^*\mathcal{B}_3^{*3} + \frac{1}{5}\mathcal{B}_3^{*5}. \tag{10}$$

In the above relations $\mathcal{B}_k^*=\mathcal{B}_k/\mathcal{B}_2$, where the second virial coefficient, $\mathcal{B}_2=B_2\Gamma_0$, with $B_2=4$ is the hard sphere second virial coefficient and $\Gamma_0\equiv\Gamma(1-3\varepsilon)$. Thus, the coefficients a_k defining function A are determined through the C function (via derivatives of the ψ function) and the first $k+1$ virial coefficients, respectively.

According to the relations $A+\ln[\Gamma(1+(C-3)\varepsilon)/\Gamma_0]=\Sigma(a_k+\frac{1}{k!}\partial^k\psi/\partial\zeta^k)\zeta^k=\Sigma w_k\zeta^k$, the generic equation, Eq. (3) can also be equivalently expressed as follows:

$$Z(\zeta,n) = \mathcal{B}_2\zeta e^{W}, \tag{11}$$

where the W function is defined

$$W(\zeta,\varepsilon) = \sum_{k=1}^{\infty} w_k\zeta^k. \tag{12}$$

There are some attractive features of the formula in Eq. (11). It involves only the virial coefficients and its expansion is the virial series. Consequently, a description of the dense region of the softer particle fluid should become more feasible than with the formula given in Eq. (3). In principle, using (11) a simple and straightforward calculation of $Z(\zeta)$ for any n is possible. However, current knowledge is usually limited to the lowest virial coefficients, and the overall performance of Eq. (11) with a truncated series representation of

the W function has to be verified against "exact" computer simulation results, which is a subject in the next section. Note also that the formula in Eq. (11) is derived from a formula which is itself a direct consequence of the local scaling property of the inverse-power fluid, Eq. (2). Thus, it should not be considered merely an acceleration method for the virial series. In the hard-sphere limit $\mathcal{B}_k$ reduces to the corresponding hard-sphere virial coefficient, B_k, and the conditions $\Gamma[1+(C-3)\varepsilon]=\Gamma_0=1$ and $W\equiv A\equiv A_{HS}$ are satisfied. This limiting case, $Z_{HS}=B_2\zeta\exp(A_{HS})$ and its application for hard hypersphere fluids will be discussed in a separate publication.

The local scaling property of the cavity function [in Eq. (2)] yields an equivalent form for the equation of state,

$$Z(\zeta,n)=4\zeta g_{max}\Gamma\left(1-\frac{3}{n}+x\right)x^{-x}e^{x}, \tag{13}$$

where $x\equiv r_{max}^{-n}$ and r_{max} is the distance at which the first peak of the radial distribution function has its maximum value, $g_{max}\equiv g(r_{max})$. In deriving the above formula we first note that the extremum condition $dg/dr=0$ for $g=y\exp(-u)=\exp(A-1/r^n)/r^C$ in the particle contact region yields $r_{max}=(n/C)^{1/n}$. Next we consider the relation $g(r_{max})=\exp(A-1/r_{max}^n)/r_{max}^C$. In this relation the term $\exp(A)$ is replaced by an expression obtained from rearranging the formula (3). Substituting $r_{max}=x^{-1/n}$ and $C/n=x$, and after some rearrangement the formula (13) is recovered. The above relation in Eq. (13) is a formula which shows that the two characteristic features of the radial distribution function, the position and height of its first peak, are sufficient to specify the equation of state of the inverse-power fluid as well. The formula in Eq. (13) has the advantage that it casts the soft-sphere equation of state in terms of the same quantities required for the hard-sphere case, so the transition between the two is clearly evident. In the hard-sphere limit $r_{max}\to 1$ (or $x\to 0$), and the height g_{max} is the only remaining system parameter of relevance, and the well-known formula $Z_{HS}=4\zeta g_{max}$ is recovered.

III. $W(\zeta,\varepsilon)$ FUNCTION

To obtain the W function [defined in Eq. (12)] information on the virial coefficients is necessary. The second virial coefficient is known for any n and $\mathcal{B}_3$ can be calculated numerically to any desired accuracy from the double integral formula [18]. A general scheme for evaluating $\mathcal{B}_4(\varepsilon)$ was proposed in Ref. [18] and the exact coefficients have been computed for several ε values [19]. Recently, virial coefficients up to the seventh have been calculated by Wheatley [20] for a large number of hardnesses, $n\geqslant 5$. Calculations of higher virial coefficients is a nontrivial and demanding task, and B_{10} for hard spheres seems be the current limit [21].

In this situation it is necessary to consider the W function as the sum of truncated series and a remainder part: $W=\sum_{k=1}^{M}w_k\zeta^k+R$. The performance of the scheme based on Eq. (11) relies on the relative contribution of the R part. The scheme may be expected to be especially useful if R is negligible or can be approximated by some effective function, R^* such that,

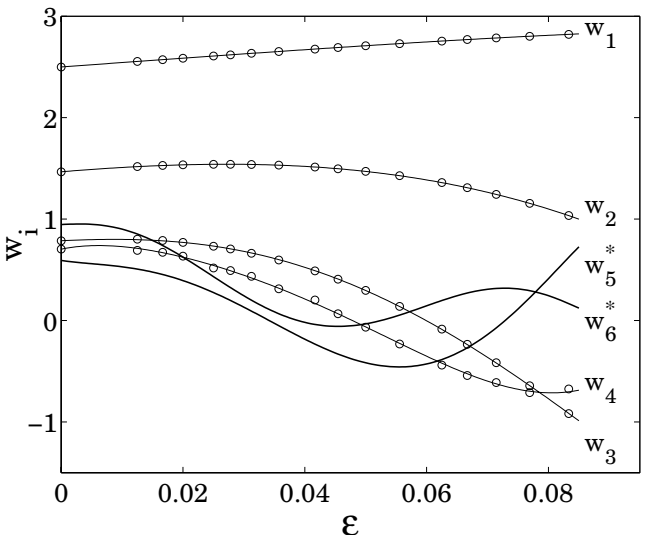

FIG. 1. The expansion coefficients of the polynomial representation of the W function, from Eqs. (14) and (15) for the equation of state formula given in Eq. (11). The first four coefficients are calculated from formulas in Eqs. (6)–(9) (the open circles). The two effective coefficients, w_5^*, w_6^* were estimated by fitting to the simulation data. The solid lines are the polynomials given in Eqs. (16) with the coefficients given in Table I.

$$W\cong W^*=\sum_{k=1}^{M}w_k\zeta^k+R^*. \tag{14}$$

Wheatley's results allow evaluation of the w coefficients from the relations Eqs. (6)–(10), and they are presented in Fig. 1. The values at $\varepsilon=0$ are calculated with the hard sphere virial coefficients (up to B_8) which are known with great precision [21]. The precision of $\mathcal{B}_7(\varepsilon)$ is considerably lower than the remaining virial coefficients and w_5, evaluated from Eq. (10), does not allow us to make convincing and sufficiently accurate predictions for Z at higher densities. Thus, instead of an exact w_5 an adjustable or effective coefficient w_5^* is presented in the figure which was defined by taking,

$$W^*=w_1\zeta+w_2\zeta^2+w_3\zeta^3+w_4\zeta^4+w_5^*\zeta^5+w_6^*\zeta^6, \tag{15}$$

i.e., by choosing $M=4$ and $R^*=w_5^*\zeta^5+w_6^*\zeta^6$ in Eq. (14).

The effective functions, w_5^*, w_6^* were obtained from least square fitting of the simulation data for the equation of state, Z_{simul} by $\mathcal{B}_2\zeta\exp(W^*)$. The simulation data employed in this work were obtained using the procedures discussed in [22]. Equilibrium MD simulations were carried out at a reduced temperature, $k_BT/\epsilon=1$ for a range of densities with the potential given in Eq. (1), and n values ranging between 12 to 1152 on $N=500$ and 864 particle systems. The simulations were carried out typically for 5–100 million time steps of duration 0.005 to $0.000\,08\sigma(m/\epsilon)^{1/2}$ for $n=12$ to 1152, respectively.

The six functions presented in Fig. 1 are well represented by polynomials

TABLE I. The coefficients q_{ik} of the polynomials representing the w_i defining the function $W^*=\Sigma_{i=1}^{4} w_i\zeta^i+w_5^*\zeta^5+w_6^*\zeta^6$, as specified in Eqs. (15) and (16). See also Fig. 1.

k	q_{1k}	q_{2k}	q_{3k}	q_{4k}	q_{5k}^*	q_{6k}^*
0	2.5000	1.466192	0.786448	0.703509	0.591899	0.946288
1	4.315199	4.966352	2.807957	12.373260	−8.600388	2.641428
2	1.102407	−63.043073	−108.021589	−1239.554954	716.765765	−35.061245
3	−68.605091	−683.394353	−4184.078357	29627.659443	−57650.578963	−98983.058566
4	−132.784961	−308.316390	25999.144890	−507009.517669	1028209.454366	3449140.704714
5	0.0	1041.903458	2936.281030	4402831.885963	−5089322.066707	−40674110.064717
6	0.0	−5393.010046	−89724.884753	−12596730.350600	0.0	160197762.582475

$$w_i = \sum_{k=0}^{6} q_{ik}\varepsilon^k, \tag{16}$$

where $i=1,2,\ldots,6$. The coefficients q_{ik} are given in Table I. It is worth noting that the effective w_5^* agree quite well with the w_5 or, as can be seen in Fig. 2, the corresponding effective seventh virial coefficient agree well with $\mathcal{B}_7(\varepsilon)$ obtained by Wheatley [20].

The equation of state formula (11) with six w coefficients given in Fig. 1 represents the simulation compressibility factors at densities even close to the freezing density with an accuracy $|Z-Z_{simul}|<0.006$, and for most of the ζ, ε points the agreement is better than 0.1 percent, which is sufficient for most practical applications. Furthermore this formula correctly describes the low density behavior of $Z(\zeta,\varepsilon)$, reproducing in its density expansion the first six virial coefficients.

Therefore an explicit equation of state formula for the soft-sphere fluid has been obtained which gives an accurate representation of the thermodynamic properties of the inverse-power fluid and correctly describes its low density behavior. This is the formula given in Eq. (11) with $W\cong W^*$ from Eq. (15) and Eq. (16) with the necessary coefficients given in Table I. Details of the $Z(\zeta,\varepsilon)$ surface are discussed in Sec. IV.

The form of the w functions in Fig. 1 indicates, that a considerable contribution to Z, for any considered softness, should come from the first two coefficients. In fact $\mathcal{B}_2\zeta\exp(w_1\zeta+w_2\zeta^2)$ provides a very good representation of $Z(\zeta,\varepsilon)$ at low and intermediate packing fractions, $\zeta<0.4$. For the dense fluid region the approximation $W^*=w_1\zeta+w_2\zeta^2$, i.e., $M=2, R^*\equiv 0$ is not sufficient to give a convincing agreement with Z_{simul}. However, for small ε the w_k functions are positive and slowly decreasing with k and a systematic convergence towards Z_{simul} is observed with increasing M and $R^*\equiv 0$. Furthermore, in the case of the hard spheres ($\varepsilon=0$), $M=8$ is sufficient to reproduce Z_{simul} with an accuracy better than 0.005. Also, as is visible in Fig. 1, for softer potentials, the w_k are rather small and change in sign for higher $k>2$. The above strongly suggests that knowledge of the virial coefficients up to ten may be sufficient to describe the $Z(\zeta,\varepsilon)$ surface with great precision in the entire fluid phase without any adjustable parameters.

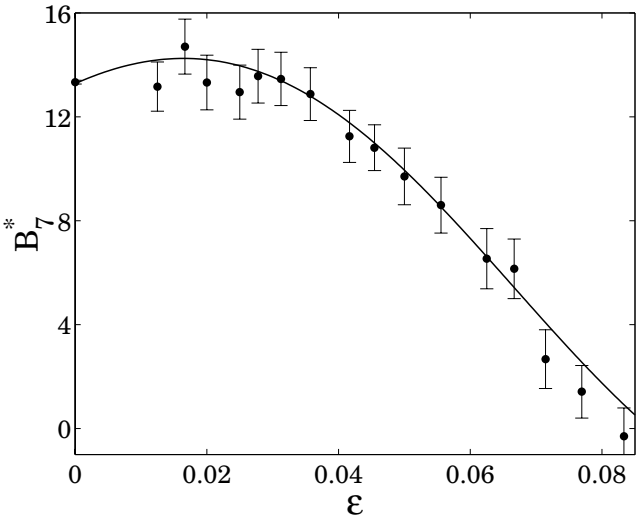

FIG. 2. The seventh virial coefficient of the inverse power fluid. The dots with error bars are values calculated by Wheatley [20]. The line is from the relation in Eq. (10) with the effective w_5^* from Fig. 1.

IV. $Z(\zeta,\varepsilon)$ SURFACE

The range of applicability of the generic formula in Eq. (3) [and its equivalent forms in Eq. (11) and Eq. (13)] are considered first. As was mentioned above it represents the thermodynamic properties of the inverse-power fluids for $n\geqslant 12$. Presumably, by adding additional terms in the W^* or A and the C functions (discussed in the next section) this range could be extended to fluids composed of even softer particles (i.e., $n<12$). In what follows consideration is restricted to the softness range $0\leqslant\varepsilon\leqslant 0.0833$.

As the present approach relies on the spherically symmetric or only distance dependent cavity function it would not expected to be applicable to the solid. Also, the metastable fluid branch above the thermodynamic freezing point needs special attention and will not be considered here. The solid-fluid coexistence properties of inverse-power systems were investigated by Agrawal and Kofke for a very broad range of the softness parameter [23,24]. Applying the Gibbs-Duhem method, they determined the freezing density, ζ^f, and freezing pressure for a number of different values of the potential softness parameter. The simulation results for seven

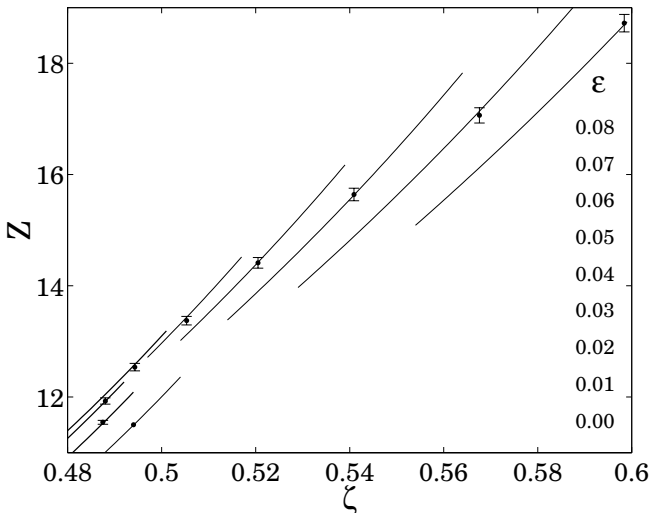

FIG. 3. The compressibility factor in the freezing region. The dots with error bars are the freezing conditions determined by Agrawal and Kofke [24]. The solid lines are from the formula given in Eq. (11) along with Eqs. (15) and (16). In the figure only parts of the full curves are shown to more clearly demonstrate the agreement with the Agrawal and Kofke data.

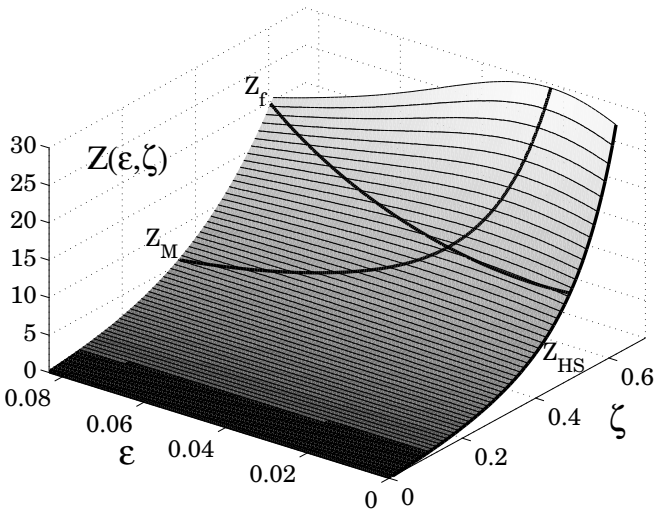

FIG. 4. The equation of state surface of the inverse power fluid, $Z(\zeta,\varepsilon)$, where $\varepsilon \equiv 1/n$. The lines in the figure are "isochors" and the bold line, $Z_M \equiv Z(\zeta^M)$, traces out the locus of their maximum values or where $(\partial Z/\partial\varepsilon)_\zeta = 0$. The limiting hard sphere line, $Z_{HS} = Z(\zeta,0)$ is the Kolafa equation. The third bold line, $Z_f \equiv Z(\zeta^f)$, is the freezing curve, with the following functional form, $\zeta^f(\varepsilon) = 1145.1049\varepsilon^4 - 204.7980\varepsilon^3 + 37.4706\varepsilon^2 - 0.9663\varepsilon + 0.4940$, obtained by fitting to the freezing line data of Agrawal and Kofke [24]. The part of the surface above the $Z(\zeta^f)$ curve is not a thermodynamically stable fluid. It is drawn to place the course of the maximum Z line in the context of the underlying phase diagram and illustrates possible behavior in the metastable region. The maximum line $\zeta^M(\varepsilon)$, for $\varepsilon > 1/34$, can be well represented by the polynomial $\Sigma_{k=0}^4 b_k \varepsilon^k$ with the coefficients $b_0 = 0.812\,694$, $b_1 = -18.489\,540$, $b_2 = 354.650\,864$, $b_3 = -3515.161\,445$, and $b_4 = 13\,700.036\,196$.

$\varepsilon \leqslant 0.08$ are shown as points in Fig. 3. The lines in this figure show predictions of the formula of Eq. (11) for the same values of ε. The two sets of data agree within statistical uncertainty, which demonstrates that the present approach is applicable up to the freezing packing fraction, i.e., $0 \leqslant \zeta \leqslant \zeta^f(\varepsilon)$ [the approach based on Eq. (4) used in [13] is less amenable to describe this dense fluid region, at least for softer systems].

The freezing point packing fractions taken from Ref. [24] are well represented by a fourth order polynomial. This gives the freezing line $\zeta^f(\varepsilon)$ and the corresponding compressibility factor freezing curve, $Z_f \equiv Z[\zeta^f(\varepsilon)]$. This freezing curve is the bold line on the $Z(\zeta,\varepsilon)$ surface in Fig. 4. Drawing the $Z(\zeta,\varepsilon)$ above the freezing curve helps appreciate some of the features of the thermodynamically stable fluid phase below this curve. It contains, as has been noticed in [13], a fold which separates the surface into two regions characterized by a positive or negative softness "compressibility," which can be defined by $\chi = (\partial Z/\partial\varepsilon)_\zeta^{-1}$. In other words to increase pressure at a given packing fraction in the one region (i.e., $\chi > 0$) the potential needs to be made softer, and to increase pressure in the second region (i.e., $\chi < 0$) it needs to be harder, by increasing n.

The demarcation line tracing out maximum pressure can be determined numerically from the condition $(\partial W/\partial\varepsilon)_\zeta = -[\partial \log(\Gamma_0)/\partial\varepsilon]_\zeta$ which is the extremum condition $(\partial Z/\partial\varepsilon)_\zeta = 0$. The demarcation or maximum compressibility factor curve is marked as "Z_M." It crosses the freezing curve at $\varepsilon \cong 0.03$ [or at about $n = 33$ and $\zeta^f(n=33) \simeq 0.494$]. This crossing point was slightly overestimated previously in [13] and roughly estimated to be $40 < n < 50$. The formula in Eq. (4) exploits three functions $(Z_{HS}, \delta A, C)$ and consequently is less accurate than formula Eq. (11) in the region close to freezing. Figure 5 shows curves of constant Z on the ζ,ε plane, where each curve terminates on the hard sphere $(\varepsilon = 0)$ line. From the condition $Z(\zeta,\varepsilon) = Z_{HS}(\zeta = 0.494) \cong 11.50$ [25], the hard sphere freezing value, the iso-Z line is obtained, which is denoted by $\zeta^{HS}(\varepsilon)$ in the figure. On the ε against ζ surface, the contours to the right of the ζ^{HS} indicate a compressibility factor of the soft-sphere fluid that is higher than that of a thermodynamically stable hard-sphere fluid. Thus, strictly speaking, for the (ζ,ε) points (states) between the ζ^{HS} and ζ^f lines, the properties of the inverse-power fluid cannot be simply mapped onto those of the hard-sphere fluid, and the formula in Eq. (4) is not directly applicable. However, as we have shown in [13], the use of $Z_{HS}(\zeta > \zeta^f)$ (i.e., in the unstable region of the phase diagram) is not entirely without foundation, and there is some evidence that the Carnahan-Starling and Kolafa formulas may describe the hard sphere equation of state reasonably accurately part way into the metastable hard-sphere fluid region [26].

Another line of interest on Fig. 5 which is referred to as the "twin" or $\zeta^t(\varepsilon)$ line here, is the solution ε for a given value of ζ for which $Z(\zeta,\varepsilon) = Z_{HS}(\zeta)$ is satisfied. This line represents the set of (ζ,ε) states which for a given packing fraction the compressibility factor of the soft-sphere fluid is the same as the hard-sphere fluid. Above the twin line, in the most dense and soft part of the diagram, there is the situation in which $(\partial Z/\partial\varepsilon)_\zeta < 0$ and $Z(\zeta,\varepsilon) < Z_{HS}(\zeta)$.

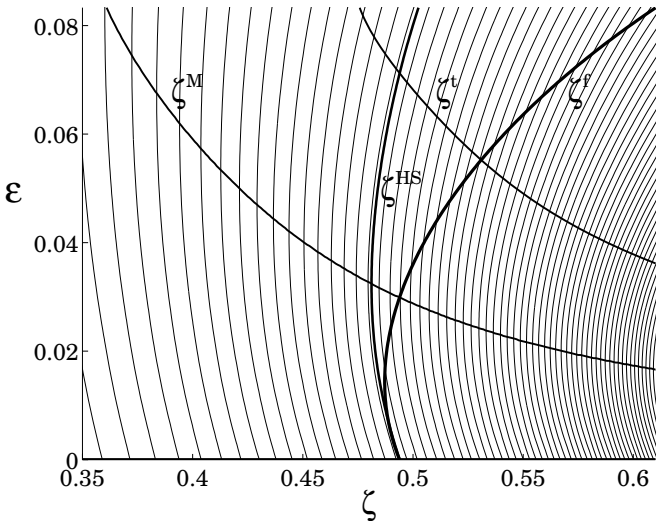

FIG. 5. Projection of a part of the equation of state surface from Fig. 4 on the density-softness plane. The curves on the figure are iso-Z lines, i.e., where $Z(\zeta,\varepsilon)$ has a constant value. The bold ζ^{HS} line, represents the iso-Z line for which $Z\cong 11.50$, i.e., the value of the compressibility factor of the hard-sphere fluid at freezing. The bold lines ζ^M,ζ^f,ζ^t are, respectively, the maximum, freezing, and twin lines.

V. $C(\zeta,\varepsilon)$ AND $A(\zeta,\varepsilon)$ FUNCTIONS

The C function has the useful feature that its dependence on n is relatively weak, and for larger n can be well-represented by its limiting form $C(\zeta,0)$, which is given in terms of the value of the derivative of the hard-sphere radial distribution function at contact, $-g(\sigma^+)^{-1}\,dg(r)/dr|_{r=\sigma^+}$. Several approximate analytical formulas have been proposed for $C(\zeta,0)$ [27,28]. Recently, using MD simulation data we have obtained for $C_0(\zeta)\equiv C(\zeta,0)$ a simple formula valid in the whole of fluid range [29],

$$C_0(\zeta) = 9\zeta(1+\zeta)(1+s_1\zeta+s_2\zeta^2+s_3\zeta^3)/(2-\zeta), \quad (17)$$

where s_1,s_2,s_3 are constants. Knowing the limiting function we propose a general expression for $C(\zeta,\varepsilon)$,

$$C(\zeta,\varepsilon) = \alpha C_0(\zeta/\alpha) + f_\varepsilon f_\zeta, \quad (18)$$

where $\alpha=\zeta^f(\varepsilon)/\zeta^f_{HS}\cong\Sigma_{k=0}^4\alpha_k\varepsilon^k$, $f_\varepsilon=\varepsilon(b_1+b_2\varepsilon+b_3\varepsilon^2)$, and $f_\zeta=(d_1+d_2\zeta+d_3\zeta^2+d_4\zeta^3+d_5\zeta^4)\zeta$.

The function α is the freezing line in $\zeta^f_{HS}=0.494$ units, so, that $\alpha(\varepsilon=0)=1$. A role of the α scaling is to exploit the limiting hard-sphere function C_0 for softer fluids for which $\zeta^f(\varepsilon)>\zeta^f_{HS}$. All necessary in Eq. (18) constants (i.e., s_k,α_k,b_k,d_k) for the $C(\zeta,\varepsilon)$ function are given in Table II. The above formula gives a good representation of the simulation data practically down to $n=12$ for the whole fluid phase density range. The empirical formula in Eq. (18), notably with the "α" scaling allows us to apply the hard-sphere expression, C_0 to soft-sphere states which are still fluid above a packing fraction of 0.494 (the hard-sphere maximum equilibrium fluid value). The relatively simple product f_ε and f_ζ in Eq. (18), splitting the ε and ζ dependence into the product of two separate functions, facilitates considerably the determination of an explicit form for C.

The C function occurs in the generic equation of state formula given in Eq. (3) indirectly, via the $(C\text{-}3)\varepsilon$ term in the argument of the gamma function. The value of this argument is close to unity for large n. Therefore the value of the gamma function is relatively insensitive to the precise nature of the ε dependence of C, at least for large n. The resulting representation of the gamma function is shown in Fig. 6 as lines, together with the simulation data values obtained from a slope of the appropriate cavity functions. Finally, with analytic expressions for C and W, an explicit form for the A function is given from $A=W-\ln[\Gamma(1+(C-3)\varepsilon)/\Gamma_0]$ from Sec. II.

As has been shown, the C function fully determines the position of the maximum of the first peak of the radial distribution function. Thus, knowing the $C(\zeta,\varepsilon)$ function the $r_{max}(\zeta,\varepsilon)$ surface is given from $r_{max}=(n/C)^{1/n}$. Figure 7 gives the softness dependence of r_{max} for several packing fractions. Also shown on Fig. 7 are some r_{max} determined directly from the radial distribution function of the soft-sphere fluid, where it can be seen that the agreement is very good. A noteworthy feature of the r_{max} surface is the presence of maximum values, defined by $(\partial r_{max}/\partial\varepsilon)_\zeta=0$, the locus of which is the bold line marked "r^M_{max}" on the figure. This indicates that for the higher packing fractions the first $g(r)$-peak position increases from a value of unity and then decreases above a certain value of increasing softness. The locus of ζ,ε points at which $(\partial r_{max}/\partial\varepsilon)_\zeta=0$ is different from those obeying the condition $(\partial Z/\partial\varepsilon)_\zeta=0$. Thus, the presence of the ridge in the Z plane is not solely a consequence of the r_{max} behavior. The maximum in Z is also not a direct consequence only of the g_{max} behavior. Knowing Z and r_{max} (or the W and C) the $g_{max}(\zeta,\varepsilon)$

TABLE II. The constants used in the definition of the C function in Eqs. (17) and (18). s_k constants are from [29], α_k are the freezing line coefficients (see the caption of Fig. 4) divided by $\zeta^f_{HS}=0.494$, and b_k,d_k are from the fitting of simulation data.

k	s_k	α_k	b_k	d_k
1	0.9799	1.0	4.3796	0.7836
2	−0.8175	−1.9560	228.8386	6.7496
3	6.4420	75.8514	−1648.5407	−16.1979
4		−414.5708		72.5301
5		2318.0261		−81.4920

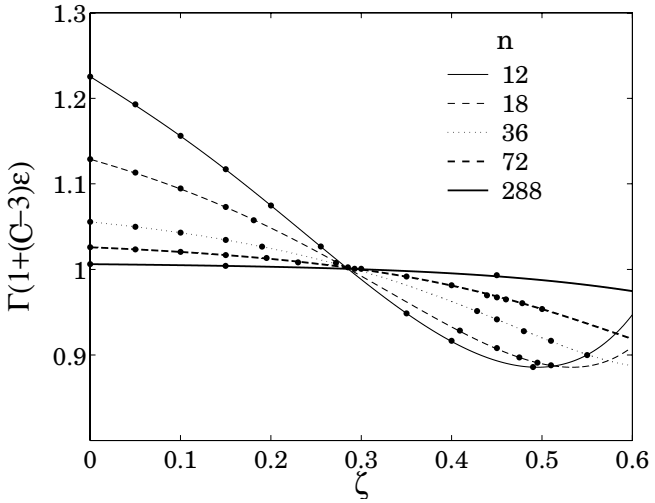

FIG. 6. Density dependence of the gamma function in the generic equation of state formula given in Eq. (3) for several values of the steepness parameter, $n=1/\varepsilon$. The solid curves are for the C function obtained from the expression in Eq. (18). Each symbol (dot) is for C from the slope of a $\log(y)$ vs $\log(r)$ plot of the MD simulation data.

surface is accessible, e.g., from Eq. (13). For any packing fraction the height of the first $g(r)$ peak monotonically diminishes with increasing softness. The $g_{max}(\zeta,\varepsilon)$ is a monotonically evolving surface without any fold or hump.

Figure 8 demonstrates that the presence of the ridge in the Z surface can be understood from the formula in Eq. (13) which can be expressed as a product of two functions $Z=g_{max}Q(r_{max})$, where $Q(r_{max})=4\zeta\Gamma(1-3\varepsilon+x)x^{-x}\exp(x)$ is

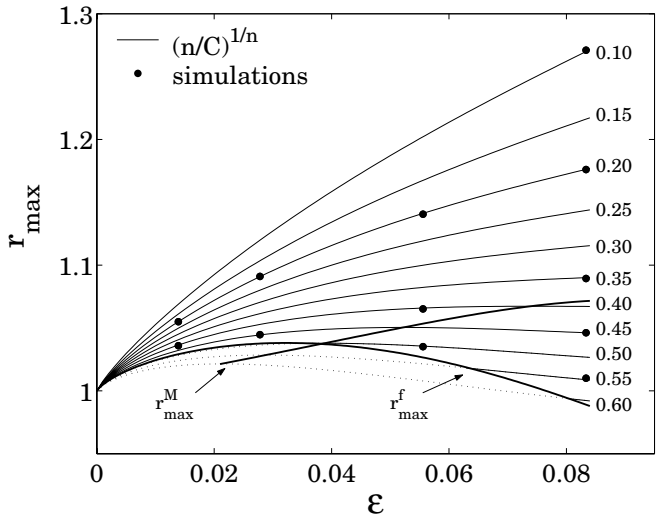

FIG. 7. The distance $r_{max}(\varepsilon)$ at which the first peak of the radial distribution function has its maximum for various packing fractions specified on the figure. The solid lines are from the relation $r_{max}=1/(\varepsilon C)^{\varepsilon}$ where C function is from Eq. (18). A few examples of r_{max} obtained directly from the MD simulations are given as dots. The line r^f_{max} traces out r_{max} at freezing. Note that the region below this line is not a thermodynamically stable fluid. The bold line r^M_{max} traces out the (ζ,ε) points for which $(\partial r_{max}/\partial\varepsilon)_\zeta=0$.

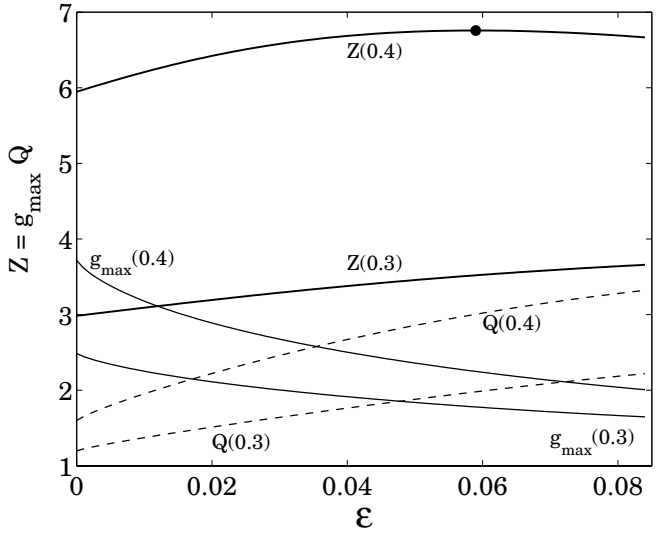

FIG. 8. In the figure the origin of the ridge in $Z(\zeta,\varepsilon)$ surface in Fig. 4 is illustrated. The g_{max} and $Q(r_{max})$ monotonically decrease and increase with softness function, respectively. As a result of these opposite tendencies their product, the Z function, has a maximum marked as a dot for $\zeta=0.4$. For $\zeta<0.36$ the maximum is formed at $\varepsilon>0.0833$ and thus, the $Z(\zeta=0.3)$ curve increases systematically within the considered softness range.

the part entirely dependent on r_{max}. It can be seen that for any packing fraction Q increases with softness (unlike r_{max} itself), whereas g_{max} decreases. Thus the opposite trends in Q and g_{max} with softness give rise to a maximum in $Z(\zeta=\text{const},\varepsilon)$. The ridge on the Z surface results from a simultaneous change in height and shift in the position of the first $g(r)$ peak with softness. Figure 8 shows the softness dependence of g_{max} and Q for two packing fractions, $\zeta=0.3$ and 0.4. The crossing of the functions moves towards larger ε with decreasing ζ. However, the ridge on the Z surface does not occur where these two functions cross, as evidenced by the fact that for $\zeta<0.36$ the maximum is not observed for the range of softness (i.e., $n\geqslant 12$) considered in this work. Nevertheless, the monotonic behavior of the Q and g_{max} functions suggests that such maximum should exist for larger ε than considered here and we expect that the ridge in Fig. 4 should continue for even softer inverse-power particles. Although as the height and sharpness of the maximum diminishes considerably on increasing softness, its precise location may be more difficult to establish for the softer particle fluids.

VI. Z-RELATED PROPERTIES

Below it is shown how a detailed knowledge of the equation of state surface $Z(\zeta,\varepsilon)$ provides direct information on some other physical quantities of the inverse-power fluid. First of all the excess free energy can be obtained from direct integration of Z over ζ as for the inverse-power fluid no liquid-gas transition occurs. Several macroscopic properties of liquids can be obtained from the integrals I_1 and I_2 defined below [30,31]:

$$I_1 = 12\zeta \int r^3 g(r) \frac{du}{dr} dr, \tag{19}$$

$$I_2 = 12\zeta \int r^4 g(r) \frac{d^2u}{dr^2} dr. \tag{20}$$

In the case of the inverse-power interaction both integrals are simply related to each other and can be expressed by the compressibility factor, i.e., $I_2=-(n+1)I_1$, and $I_1=-3Z$. As a result, explicit formulas for the (infinite frequency) second-order elastic constants [32] (in units of $\rho k_B T$) are available,

$$C_{11} = 3 + (3n+1)Z(\zeta,\varepsilon)/5, \tag{21}$$

$$C_{12} = 1 + (n+7)Z(\zeta,\varepsilon)/5, \tag{22}$$

$$C_{44} = 1 + (n-3)Z(\zeta,\varepsilon)/5. \tag{23}$$

These formulae apply in the limit of infinite frequency [32] and satisfy the Cauchy relation, $C_{44}=(C_{11}-C_{12})/2$, which reduces the number of independent elastic constants to two. From the above formulas we see that $C_{11}>C_{12}>C_{44}$, and this condition is obeyed for any n. For soft interactions the details of the ε dependence of Z surface are significant. For hard systems ($n \gg 1$) the linear n dependence becomes dominant ($Z/Z_{HS} \to 1$) and $C_{44} \simeq C_{12} \simeq C_{11}/3 \to nZ_{HS}/5$. Similar behavior is observed for the high-frequency moduli [31]. The infinite frequency elastic bulk modulus is $K_\infty = 2+nZ$, the high-frequency shear modulus is $G_\infty = 14/15+(n-3)Z/5 = C_{44}-1/15$, and the high-frequency dilation modulus $M_\infty = 3\frac{19}{45}+4(n-3)Z/15$. These moduli can therefore be placed in the relative order of magnitude, $M_\infty > K_\infty > G_\infty$ and for large steepness they all behave as $\sim nZ_{HS}$.

Also, explicit formulas for the ζ,ε dependence of the longitudinal- and transverse-wave velocities [33] can be obtained,

$$v_L = [3S(3n-1)Z(\zeta,\varepsilon)]^{1/2}, \tag{24}$$

$$v_T = [3S(n-3)Z(\zeta,\varepsilon)]^{1/2}, \tag{25}$$

where S is a constant. From Eqs. (24) and (25) it can be seen that both velocities increase with system steepness as $\sqrt{n}$. Furthermore, as expected, the longitudinal-wave velocity is for any ζ and n greater than the transverse-wave velocity, and $v_L = v_T[1+2(n+1)/(n-3)]^{1/2}$. Thus, on increasing steepness $v_L \cong v_T[3+8/n]^{1/2}$ or it goes to $v_L \cong \sqrt{3} v_T$ in the steeply repulsive limit. The ratio v_L/v_T is at a minimum in the hard sphere limit. Poission's ratio is [33],

$$\nu = \frac{v_L^2 - 2v_T^2}{2(v_L^2 - v_T^2)} = \frac{n+5}{4(n+1)} = \frac{1}{4} + \frac{19}{16n} + \cdots. \tag{26}$$

Thus, it has a minimum, $\nu_{min}=0.25$, in the hard-sphere limit and its value can be increased by making the system softer.

The local scaling property of the cavity function permits the estimation other integral derived quantities. For example there is the integral involved in the following quantities:

$$\langle u_m \rangle_n = \left\langle \frac{1}{2N} \sum_i^N \sum_j^N \frac{1}{r_{ij}^m} \right\rangle_n = 12\zeta \int \frac{1}{r^m} r^2 g(r), \tag{27}$$

where $\langle \cdots \rangle_n$ means the average over the system of N particles interacting with r^{-n} potential. With this definition $\langle u \rangle \equiv \langle u_n \rangle_n$. Using the cavity function $y=\exp(A)r^{-C}$ we derive,

$$\begin{aligned} \langle u_m \rangle_n &= 12\zeta \int Y(r) y(r) dr \\ &= 12\zeta \int \frac{1}{r^{m-2}} e^{-(1/r^n)} y(r) dr \\ &\cong 12\zeta e^A \Gamma\left(\frac{m+C-3}{n}\right). \end{aligned} \tag{28}$$

The weighting function $Y(r)$ shrinks on increasing m, so for $m>n$ the integration should be even more accurate than that for $\langle u_n \rangle_n$. For $m<n$ the above approach is less justified and the final formula represents a poorer approximation to $\langle u_m \rangle_n$, particularly for not too large n. The above formula can be written,

$$\langle u_m \rangle_n = \langle u_n \rangle_n \Gamma\left(\frac{m+C-3}{n}\right) \Big/ \Gamma\left(\frac{n+C-3}{n}\right). \tag{29}$$

Thus, knowing $\langle u \rangle = 3Z/n$ and C the quantity, $\langle u_m \rangle_n$, can be obtained. For large n this quantity is mainly determined by $\langle u \rangle$. In general, however, $\langle u_m \rangle_n$ differs from $\langle u \rangle$ and depending on m, can be smaller or larger than $\langle u \rangle$. Note that the relation in Eq. (29) is a direct consequence of the scaling property of the cavity function, and is therefore expected to work well only for $n \geqslant 18$. The quantity, $\langle u_m \rangle_n$ can be used in the calculations of properties involving derivatives of the energy, e.g., terms of the short-time expansion of different correlation functions [34], so they can also be useful in illuminating some aspects of dynamical (time dependent) properties.

VII. EFFECTIVE HARD-SPHERE DIAMETER

The effective hard-sphere diameter (EHSD) is a useful concept in liquid theory and has been widely used to calculate a number of physical properties [35,36]. Usually in the perturbation approach for liquids the reference system is the hard-sphere fluid and an appropriate choice of the EHSD (which in general depends on temperature and density) can give a good approximation of the liquid properties, at least for some parts of its phase diagram. Several different formulas have been proposed for the EHSD. Among the most frequently applied, are the criterion for the EHSD by Barker and Henderson (BH) [37] and that in the perturbation theory by Weeks, Chandler, and Andersen [38], as well as later modifications [35].

Knowledge of the $Z(\zeta,n)$ enables an explicit formula for the effective hard-sphere diameter, σ_{HS}^{ef} to be obtained which can be used to define the effective packing fraction, $\zeta_{HS}^{ef}/\zeta = (\sigma_{HS}^{ef}/\sigma)^3$. This route to EHSD follows the approach of del Rio [39] and for such a purely repulsive (with there-

fore no vapor-liquid coexistence) it seems to be the most appropriate mapping of the system's properties onto that of the HS fluid [39,20]. This fairly unique situation can then be employed in a range of applications for EHSD formulas. Also it offers a promising starting point for developing perturbation schemes based directly on the soft repulsive reference systems rather than on the HS fluid.

The effective packing $\zeta_{HS}^{ef}(\zeta,\varepsilon)$ is the solution of the following equation [39]:

$$Z_{HS}(\zeta_{HS}^{ef}) = Z(\zeta,\varepsilon). \tag{30}$$

As accurate analytic representations for the hard-sphere equation of state have been derived, an analytic solution of (30) is possible. The representation of Z_{HS} by the CS or Kolafa equation of state leads to an algebraic equation of third and fourth order in ζ_{HS}^{ef}, respectively (for algebraic equations of order less than five a general solution exists). For instance, using the CS formula then, $x^3+Q_1x^2+Q_2x-1=0$, where x stands here for ζ_{HS}^{ef}, $Q_1=-(2+3Z)/Z$ and $Q_2=(4+3Z)/Z$. Making the substitution $x=y-Q_1/3$, the equation $y^3+3py+2q=0$ is obtained, for which a general solution is available. In this equation $p=(3Q_2-Q_1^2)/9$ and $q=Q_1^3/27-Q_1Q_2/6-1/2$ and it can be confirmed that for the range of ζ and ε considered in this work, the parameter p is negative. For $p<0$, depending on the sign of $D\equiv q^2+p^3$, two different cases have to be distinguished: cases: if $D>0$, there is one real solution, and if $D\leqslant 0$ there are three possible real solutions. It was verified that here, ζ_{HS}^{ef} is composed of three solutions, which are denoted by ζ_1^{ef}, ζ_2^{ef}, and ζ_3^{ef}. For all ζ,ε such that $Z>4/3\sqrt{3}$, which is the condition $D>0$, giving,

$$\zeta_1^{ef} = (-q+\sqrt{D})^{1/3} - (q+\sqrt{D})^{1/3}. \tag{31}$$

For $Z\leqslant 4/3\sqrt{3}$ (i.e., the condition $D<0$ holds) and $Z>2\sqrt{2}/3\sqrt{3}$, we have,

$$\zeta_2^{ef} = -2\lambda\cos(\varphi/3), \tag{32}$$

and finally for the remaining ζ,ε for which the condition $D<0$ is obeyed and $Z\leqslant 2\sqrt{2}/3\sqrt{3}$, the solution is,

$$\zeta_3^{ef} = 2\lambda\cos(\pi/3-\varphi/3). \tag{33}$$

In the above equations, $\lambda=\mathrm{sgn}(p)\sqrt{|p|}$, and $\cos\varphi=q/\lambda^3$. The resulting effective packing fraction ζ_{HS}^{ef} is illustrated in Fig. 9. The derived ζ_{HS}^{ef} from Eqs. (31)–(33) provides a rigorous solution of Eq. (30), making it an essentially exact solution of effective packing fraction (or diameter) of the inverse-power fluid, covering essentially the whole of ζ,ε space.

Knowledge of the exact effective packing formula enables the various approximate EHSD representations to be tested. In particular the role of interaction softness can be studied to an extent not possible before. For example, in Fig. 10 some features of the BH criterion are demonstrated. For the inverse-power system the BH criterion gives $\zeta_{BH}=\zeta\Gamma(1-\varepsilon)^3$, which is obeyed well in the steeply repulsive limit. However, as it is clear from the figure, the BH formula quickly deteriorates with increasing system softness. As

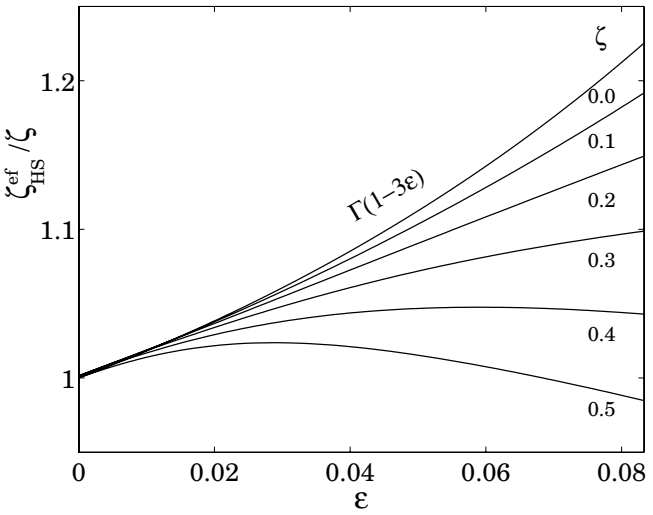

FIG. 9. The effective hard-sphere packing fraction surface, $\zeta_{HS}^{ef}(\zeta,\varepsilon)$ calculated from the condition given in Eq. (30) and illustrated for selected packing fractions. The surface is composed of three parts given by the formulas in Eqs. (31)–(33).

expected for the BH criterion, the density dependence of the ζ_{HS}^{ef} is not taken properly into account. It is interesting to observe that there exists a particular range of packing fractions close to $\zeta=0.139$ for which ζ_{BH} (or equivalently σ_{BH}) represents almost exactly the ζ_{HS}^{ef} (the horizontal dotted line in Fig. 10). In other words for a small range of packing fractions the properties of the inverse-power fluid are very well represented by the BH formula, $Z(\zeta\simeq 0.139,\varepsilon)\cong Z_{HS}(\zeta_{BH})$. Also, from Fig. 10 it may be seen that in general the BH criterion overestimates the "true" ζ_{HS}^{ef} (or $\sigma_{BH}>\sigma_{HS}^{ef}$). For dilute systems ($\zeta<0.139$), however, the BH criterion underestimates the ζ_{HS}^{ef} (or $\sigma_{BH}<\sigma_{HS}^{ef}$). More importantly, this

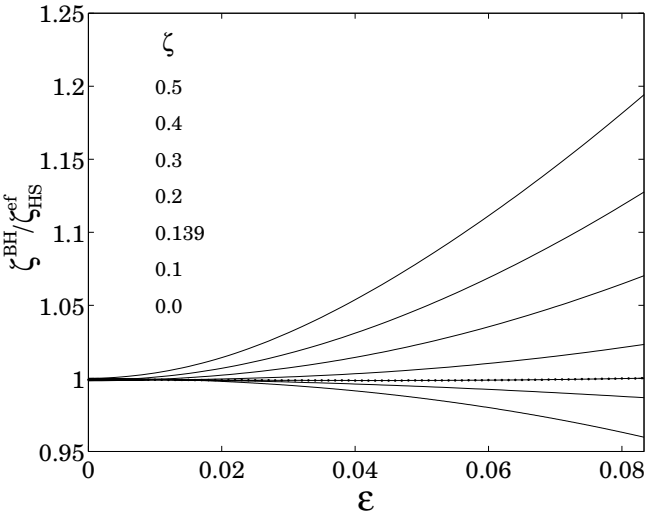

FIG. 10. The ε dependence of the Barker-Henderson effective packing fraction, ζ^{BH} compared to the exact effective packing fraction, ζ_{HS}^{ef} given in Fig. 9, at several packing fractions indicated on the figure. The dotted line is for a particular packing fraction close to $\zeta=0.139$ for which the BH criterion practically coincides with the exact solution, or $Z_{HS}[\zeta^{BH}(\varepsilon)]\cong Z_{HS}[\zeta_{HS}^{ef}(\varepsilon)]=Z(\zeta,\varepsilon)$.

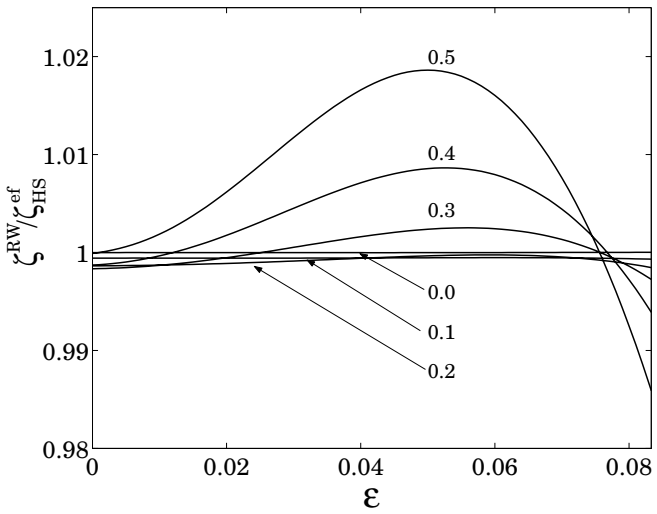

FIG. 11. Comparison of the effective packing fraction, $\zeta^{RW}=d^3\zeta$ [20] with the exact effective packing fraction, ζ_{HS}^{ef} (see Fig. 9) for the inverse power fluids illustrated at several packing fractions which are given on the figure. The effective hard-sphere diameter, d, is from the expansion up to the second order given in Ref. [20].

behavior takes place for any ε, even in the steeply repulsive limit. Therefore, $\zeta\cong 0.139$ is a demarcation line valid at all softnesses. The lowest line in Fig. 10 is the function $\Gamma(1-\varepsilon)^3/\Gamma(1-3\varepsilon)$, which is the limit $\zeta\to 0$. This limiting function has a value $\leqslant 1$, and can be recovered from the virial expansion or the low density limit of ζ_3^{ef}. The behavior of the ratio $Z_{HS}(\zeta_{BH})/Z_{HS}(\zeta_{HS}^{ef})$ is qualitatively similar to that of $\zeta_{BH}/\zeta_{HS}^{ef}$ in Fig. 10. Thus, in general the BH approach overestimates the equation of state Z of the inverse-power fluid, but in the dilute region, $\zeta<0.139$, it underestimates it.

In Fig. 11 some features of the EHSD approach recently proposed by Wheatley [20] are illustrated. It is apparent from the figure that it works very well for harder systems. Furthermore, it practically coincides with "exact" ζ_{HS}^{ef} for low packing fractions. However, some overestimation starts for $\zeta>0.3$ and for most of the softness range.

VIII. CONCLUSIONS

In this work equation of state formulas for the inverse-power fluid are proposed which are obtained solely from the scaling relation found for the cavity function of this system. The basic equation of state Eq. (3) can be recast into another form, i.e., Eq. (4), in which the cavity function scaling relation parameters, $A(\zeta,\varepsilon)$, and $C(\zeta,\varepsilon)$ are incorporated in two terms that multiply the usual hard-sphere equation of state. This formula has the advantage that the limiting hard-sphere part Z_{HS}, for which accurate representations exist, can be used directly. It is particularly useful for steeply repulsive fluids.

Another derived form of the equation of state, Eq. (13), demonstrates that the compressibility factor of the inverse-power fluid can be completely defined in terms of two well-defined characteristic features of the radial distribution function, namely the position r_{max} and height g_{max} of its first peak. (For the hard sphere, g_{max} is the only parameter to be determined.) The short-time expansion of the configurational property time correlation functions are also therefore determined (via $\langle u_m\rangle_n$) by only two structural parameters of the fluid [22].

The equation of state can also be expressed as an exponential function of an appropriate combination of the virial coefficients Eq. (11). It is simple and straightforward to apply this formula, and it can be systematically improved with increasing knowledge on the virial coefficients of the inverse-power fluid. Exploiting the five coefficients and additionally two effective functions, this formula gives an accurate representation of the compressibility factor, $Z(\zeta,\varepsilon)$, of the inverse-power fluid for an appreciable steepness parameter (for $n>12$) and density range. It represents correctly the inverse-power fluid in the dilute density region, as well as close to the freezing point. It has also allowed, for the first time, a detailed characterization of the role of the "softness" parameter. In particular we have shown that there is curve marking out a maximum value of the compressibility factor on the packing fraction and softness parameter plane (first discussed in a preliminary report of this study in Ref. [13]). It suggests that the pressure of real soft particle fluids could be controlled *in situ*, say by chemical means or by the application of an external field, which controlled the particle's degree of softness.

A detailed knowledge of the $Z(\zeta,\varepsilon)$ surface allows explicit formulas for several thermodynamic quantities (see Sec. V) to be obtained, revealing their dependence on the softness of the potential. In addition to the thermodynamic quantities, the scaling property of the Z surface, enables some aspects of dynamic properties [e.g., Eq. (29)] to be analyzed, which could be exploited in studies of the short-time expansion of the force autocorrelation function, [34], for example. Furthermore, by in a sense, "reversing" the direction of the analysis, knowledge of Z and C, enables the local structural characteristics $g_{max}(\zeta,\varepsilon)$, and $r_{max}(\zeta,\varepsilon)$ of the inverse-power fluid to be obtained in analytic form. From these forms, for example, the nonmonotonic character of the position r_{max} on increasing softness has emerged and the origin of the ridge on the Z surface can be deduced.

The effective hard-sphere diameter or packing fraction derived in Sec. VII could offer a useful foundation for testing different effective (hard sphere) diameter approaches. The comparison performed here of the Barker-Henderson approach with this work's EHSD result revealed, for example, the existence of a demarcation line for packing fractions $\zeta\approx 0.139$. For lower densities the Barker-Henderson approach underestimates the effective hard-sphere packing fraction for all values of the softness. Wheatley's EHSD approach
performed well for most of the density-softness states.

The accurate analytic expressions for the thermodynamic properties, particularly for the compressibility factor as a function of packing fraction and interaction softness, obtained in this work should make the inverse power fluid more attractive as a model reference system for real molecular fluids.

ACKNOWLEDGMENTS

A.C.B. and D.M.H. thank the Royal Society (London) and the Polish Academy of Sciences for funding this collaboration. The work has been partially supported by the Polish Ministry of Education and Science. D.M.H. thanks the Engineering and Physical Sciences Research Council of Great Britain (EPSRC) for funding workstations used to carry out some of simulations used for the work.

[1] W. G. Hoover, S. G. Gray, and K. W. Johnson, J. Chem. Phys. **55**, 1128 (1971).
[2] P. Hutchinson and W. Conkie, Mol. Phys. **24**, 567 (1972).
[3] E. La Nave, F. Sciortino, P. Tartaglia, M. S. Shell, and P. G. Debenedetti, Phys. Rev. E **68**, 032103 (2003).
[4] M. Ross, J. Chem. Phys. **71**, 1568 (1979).
[5] J.-P. Hansen and I. McDonald, *Theory of Simple Liquids*, 2nd edition (Academic Press, London, 1986).
[6] J. Dufty and M. H. Ernst, Mol. Phys. **102**, 2123 (2004).
[7] F. de J. Guevara-Rodriguez and M. Medina-Noyola, Phys. Rev. E **68**, 011405 (2003).
[8] A. C. Brańka and D. M. Heyes, Phys. Rev. E **69**, 021202 (2004).
[9] J. Zhang, J. Am. Chem. Soc. **126**, 7908 (2004).
[10] B. H. Tam, K. Tam, Y. C. Lam, and C. B. Tan, J. Rheol. **48**, 915 (2004).
[11] F. Lo Verso, M. Tau, and L. Reatto, J. Phys.: Condens. Matter **15**, 1505 (2003).
[12] J. Mewis, W. J. Frith, T. A. Strivens, and W. B. Russel, AIChE J. **35**, 415 (1989).
[13] A. C. Brańka and D. M. Heyes, Mol. Phys. **102**, 2049 (2004).
[14] I. Gradshteyn and I. Ryzhik, *Table of Integrals, Series, and Products* (Academic Press, New York, 1980).
[15] M. Miandehy and H. Modarress, J. Chem. Phys. **119**, 2716 (2003).
[16] N. F. Carnahan and K. E. Starling, J. Chem. Phys. **51**, 635 (1969).
[17] T. Boublik and I. Nezbeda, Collect. Czech. Chem. Commun. **51**, 2301 (1986).
[18] J. A. Barker, P. J. Leonard, and A. Pompe, J. Chem. Phys. **44**, 4206 (1966).
[19] M. Dixon and P. Hutchinson, Mol. Phys. **38**, 739 (1979).
[20] R. J. Wheatley, J. Phys. Chem. B **109**, 7463 (2005).
[21] S. Labik, J. Kolafa, and A. Malijevský, Phys. Rev. E **71**, 021105 (2005).
[22] D. M. Heyes, G. Rickayzen, and A. C. Brańka, Mol. Phys. **102**, 2057 (2004).
[23] R. Agrawal and D. A. Kofke, Phys. Rev. Lett. **74**, 122 (1995).
[24] R. Agrawal and D. A. Kofke, Mol. Phys. **85**, 23 (1995).
[25] J. Kolafa, S. Labik, and A. Malijevský, Phys. Chem. Chem. Phys. **6**, 2335 (2004).
[26] M. J. Maeso, J. R. Solana, J. Amoros, and E. Villar, J. Chem. Phys. **94**, 551 (1991).
[27] M. F. del Rio and A. L. Benavides, Mol. Phys. **72**, 307 (1991).
[28] F. M. Tao, Y. Song, and E. A. Mason, Phys. Rev. A **46**, 8007 (1992).
[29] D. M. Heyes, M. Cass, A. C. Brańka, and H. Okumura, J. Phys.: Condens. Matter **18**, 7553 (2006).
[30] P. Schofield, Proc. Phys. Soc. London **88**, 149 (1966).
[31] P. Egelstaff, *An Introduction to the Liquid State* (Clarendon Press, Oxford, 1992).
[32] S. Hess, M. Kröger, and H. Voigt, Physica A **250**, 58 (1998).
[33] R. V. Gopala Rao and R. Venkatesh, Phys. Rev. B **39**, 9467 (1989).
[34] A. C. Brańka and D. M. Heyes, Mol. Phys. **103**, 2359 (2005).
[35] C. M. Silva, H. Liu, and E. A. Macedo, Ind. Eng. Chem. Res. **37**, 221 (1998).
[36] Y. Tang, J. Chem. Phys. **116**, 6694 (2002).
[37] A. J. Barker and D. Henderson, J. Chem. Phys. **47**, 4714 (1967).
[38] H. C. Andersen, J. D. Weeks, and D. Chandler, Phys. Rev. A **4**, 1597 (1971).
[39] F. del Rio, Mol. Phys. **76**, 29 (1992).